Laser Composite Surfacing of a Magnesium Alloy with Chromium Carbide

J. Dutta Majumdar[a*], R. Galun[aa], B. L. Mordike[aa], B. Ramesh Chandra[a] and I. Manna[a]

[a]*Dept. of Met. & Mat. Engg., Indian Institute of Technology, Kharagpur, WB-721302, India*
[aa]*IWW, Agricola Strasse 6, D-38678 Clausthal-Zellerfeld, Germany*

The present study concerns improving the wear resistance of a Mg alloy (MEZ) by melting the surface with a high power laser and simultaneously injecting hard particles, of $Cr_2C_3 + (25\,\mu m - 40\,\mu m)$ into the surface. The laser processing was carried out using a continuous wave CO_2 laser, Model: Rofin Sinar, RS 10000, with a beam diameter of 4 mm and a focal point 30 mm above the surface. Following laser processing, a detailed investigation of the microstructures, compositions and phases were undertaken and mechanical (wear resistance) and electrochemical (pitting corrosion resistance) properties of the surface layer were evaluated in details. The microstructure of the surface layer consists of uniformly dispersed Cr_2C_3 precipitates in grain-refined matrix. The micro-hardness and wear resistance of the surface layer were significantly improved as compared to the base metal.

Key words: magnesium, chromium carbide, micro-hardness, wear, corrosion.

INTRODUCTION

Mg and its alloys are of great interest in the field of automotive and aerospace industries because of their low density (from 1.75 to 1.85 g/cm³) and high specific strength [1]. However, a relatively poor resistance to wear is a serious impediment against wider application of Mg alloys. Wear is essentially a surface related degradation, which can be reduced or minimized by an appropriate tailoring of the surface microstructure and or composition [2]. Ceramic materials are often used as wear resistant coatings due to their ultra high hardness and wear resistance [3]. However, the

---

*Corresponding Author: E-mail: jyotsna@metal.iitkgp.ernet.in

processes are limited by the extremely slow deposition and the necessity to work in vacuum and weak coating-substrate interfaces. In contrast, hard ceramic particles may be introduced on the surface by melting the surface layer with a high power laser beam and subsequent directing ceramic particles into the molten zone to produce a thin composite surfaced layer [4]. The process may be termed laser composite surfacing (LCS). During the process, melting and solidification occur within a very short time and remain confined to a thin layer the bulk acts as an infinite heat sink. There is a large temperature gradient across the boundary between the melted surface and the underlying substrate, resulting in rapid self-quenching rates as high as 10^5 K/s with concomitant solidification speeds up to 30 m/s [5–7]. In addition, the short processing time, economy in energy/material consumption, shallow heat affected zone and precision are the advantages of LCS over the conventional processes [5, 6]. In the past, several attempts have been made to enhance the wear and corrosion resistance of magnesium and its alloys by laser surface engineering [8–10]. Laser composite surfacing of MEZ with SiC and Al+Al$_2$O$_3$ was found to form a coherent and defect free composite surface with a significant enhancement of microhardness and wear resistance [11–12].

In the present study, an attempt has been made to enhance the wear resistance of a Mg alloy (MEZ) by laser composite surfacing with chromium carbide. A detailed characterisation of the laser processed zone in terms of microstructure, composition and phases has been undertaken to optimise the laser processing parameters. Finally, the mechanical, mainly micro-hardness, wear resistance and corrosion properties in an NaCl solution of the composite surface layer have been evaluated in detail.

EXPERIMENTAL

MEZ (RE 2%, Zn 0.5%, Mn 0.1%, Zr 0.1% and the rest Mg), was chosen as substrate material, because of its potential scope for application in automotive components in engine and transmission section.

Laser composite surfacing was carried out with a 10 kW continuous wave (CW) CO$_2$ laser (Model: Rofin Sinar, RS 10000) with a beam diameter of 4 mm and a focal point 30 mm above the surface by melting the MEZ substrate and simultaneously feeding Cr$_2$C$_3$ powers with a particle size $+25\mu$m–60μm. The specimens were mounted on a water chilled copper of block placed on a CNC controlled X-Y stage which could be moved at speeds of 100–400 mm/min. The relative speed between the laser beam and the specimen was maintained to control the substrate-laser beam interaction time. In order to achieve micro-structural and compositional homogeneity of the laser treated surface, a 25% overlap between successive melt tracks was necessary. The main process variables were the incident laser power (P = 1 to 4.5 kW), scan speed (v = 100 to 800 mm/min) and powder

feed rate (F_p = 16 to 30 mg/s). The angle between the powder nozzle and the specimen was maintained at 50°. Ar was used as shrouding gas and the gas flow rate was maintained constant at 6 l/min. Following LCS, the microstructure of the composite layer was characterised by optical and scanning electron microscopy. The area fraction of precipitates was measured by a standard point count technique [13]. A detailed analysis of the phase and composition of the composite layer were carried out by X-ray diffractometer and energy dispersive spectroscopic analyser, respectively. The microhardness of the composite surface layer was measured using a Vickers micro-hardness tester with an applied load of 300 g. The wear resistance of the composite surface was compared with that of the as-received MEZ by a Pin-on-Disc wear testing machine against a hardened steel disc at an applied load of 3 kg and sliding speed of 300 rpm. Finally, the effect of composite surfacing on the pitting corrosion behaviour was also studied by calculating the corrosion rate derived from the potentiodynamic anodic polarisation study in an NaCl solution, using a standard calomel electrode as reference electrode and platinum as counter electrode [14].

RESULTS AND DISCUSSIONS

Characterization of the Surface Layer

Laser composite surfacing is conducted by feeding hard chromium carbide (Cr_3C_2) particles during melting of the substrate surface with a high power laser. Hard particles are distributed instantaneously in the molten pool during laser melting and form the composite layer on the surface on solidification. Due to the large difference in physical and thermal properties of the Cr_3C_2 particles and MEZ, the choice of suitable process parameters is crucial to achieve a homogeneous microstructure. Figures 1 (a, b) show the microstructures of the (a) cross section and (b) top surface of the laser surface composite with chromium carbide produced with P = 2 kW, v = 200 mm/min and F_p = 20 mg/s. Figure 1(a) shows that the
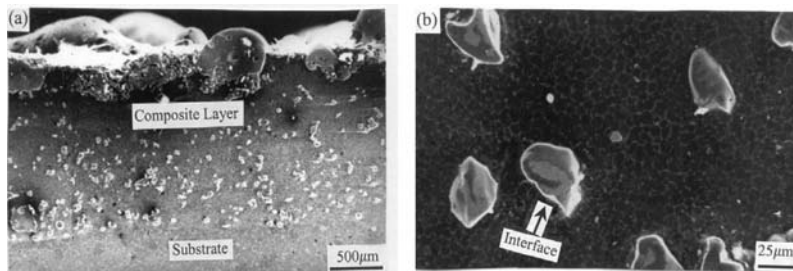

FIGURE 1
Scanning electron micrograph of the (a) cross section and (b) top surface of laser composite surface with Cr_2C_3 at a power of 2 kW, scan speed of 200 mm/min and powder feed rate of 20 mg/s.
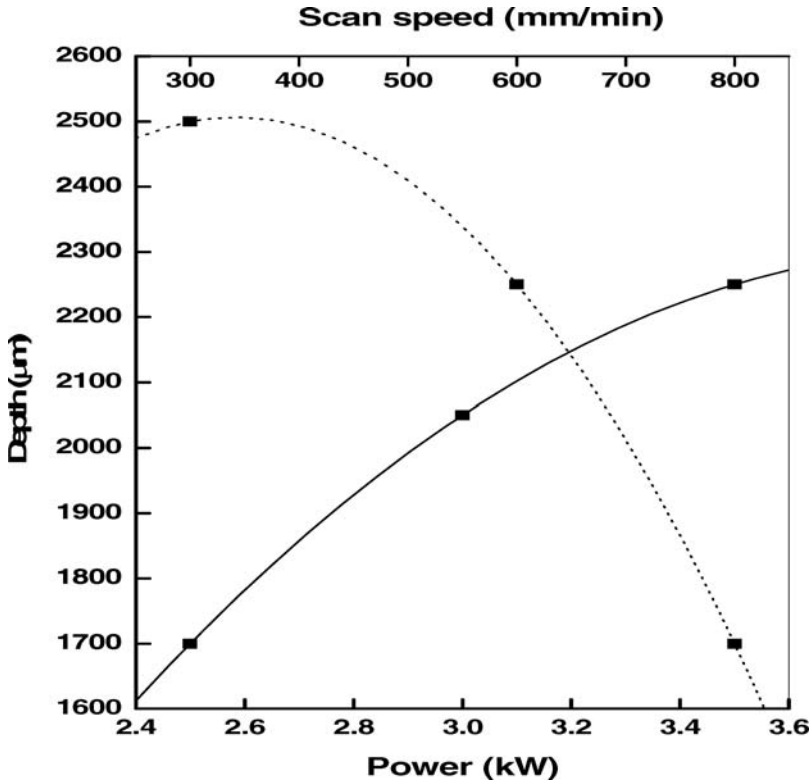
FIGURE 2
Variation of the depth of the composite layer with the applied power (solid line, at a scan speed of 300 mm/min) and scan speed (broken line, at a power of 4.5 kW for the laser composite surface with chromium carbide.

microstructure consists of uniformly dispersed chromium carbide particles in a grain refined MEZ matrix. Furthermore, the composite layer-substrate interface is defect free. However, an agglomeration of carbide particles near to the surface region should be noted. This is mainly attributed to a very high rate of quenching in the near surface region, which hinders the distribution of particles. Figure 1(b) shows that the scanning electron micrograph of the top surface of the composite surface with chromium carbide as shown in Figure 1(a). Figure 1(b) shows that the particles size varies from $25 - 35 \mu m$, which is almost same as that of the as-received powder. The distribution is uniform and the interface between the particle and matrix, as shown by the arrowhead, is adherent and defect-free. Figure 2 shows the variation of the depth of the composite layer with the applied power and scan speed for the laser composite surface. Figure 2 shows that the depth of the composite layer increases with an increase in applied

power mainly because of the increased energy absorbed at the surface. On the other hand, the depth of the composite layer decreases with an increase in the scan speed because of the reduction of the interaction time. Hence, it may be concluded that the depth of the composite layer can be controlled by a suitable selection of applied power and scan speed. Figure 3 shows the X-ray diffraction profiles of the top surface of (a) as received and (b) the laser composite surface with chromium carbide produced with a power of 2 kW, scan speed of 200 mm/min and powder feed rate of 20 mg/s. A comparison between Figure 3(a) and Figure 3(b) shows that there is a number of Cr_3C_2 peaks present together with the presence of Mg and intermetallics of Mg and rare earth elements, which is typical in as-received MEZ). Hence, it may be concluded that there is negligible/no dissociation of Cr_3C_2 particles during the process. Figure 4 summarises the variation of the area fraction of chromium carbide particles with the applied laser power (graph 1, at a scan speed of 450 mm/min) and scan speed (graph 2, at a power of 2.5 kW) for the laser composite surface with chromium carbide. In Figure 4 plot 1, firm line; at a scan speed of 450 mm/min and powder feed rate of 20 mg/s it is shown that the increase in incident laser power decreases the area fraction of particles mainly because of the increased dilution resulting from the greater depth of melting. On the other hand, the area fraction of precipitates increases with the decrease in scan speed, mainly due to an increased amount of particles fed into the pool during laser processing when the interaction time is high c.f. plot 2, dotted line; at a power of 2.5 kW and powder feed rate of 20 mg/s. Similarly, at a very high interaction time, the powder input is very low leading to almost no change in the area fraction of particles with a further increase in scan speed. Although the depth of the composite layer and the area fraction of particles were found to vary with the laser parameters, application of too high a power, or too low a scan speed, leads to the formation of surface craters due to the vaporisation of low melting Mg. Similarly, the application of a very low power or very high scan speed leads to non-uniform intermixing and hence, an inhomogeneous distribution of particles. Hence, a combination of laser power and scan speed should be carefully chosen to achieve a homogeneous microstructures. It was observed that a homogeneous and defect-free microstructure can be formed only under a narrow processing window as summarised in Table 1.

TABLE 1
Optimum laser parameters for the laser composite surface with chromium carbide.

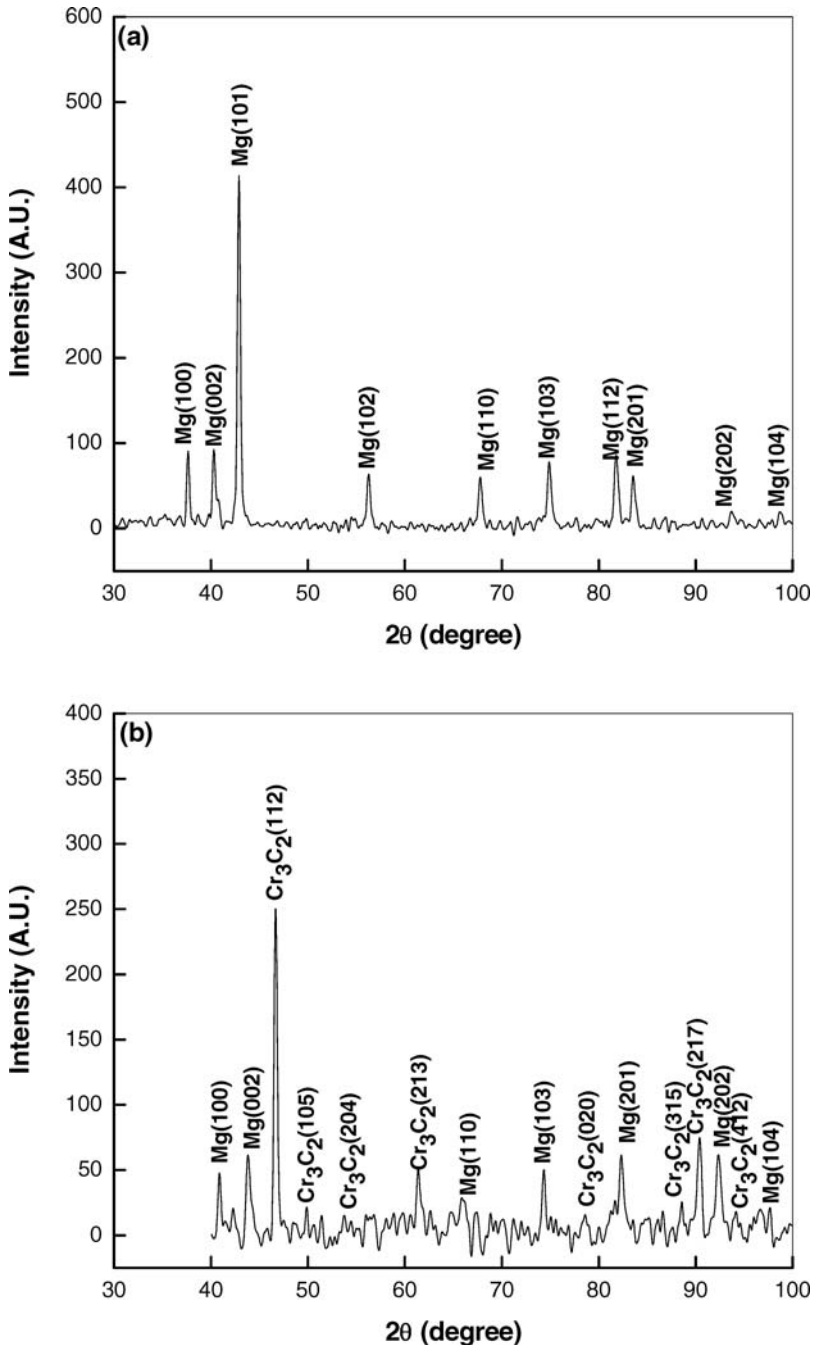| Power (kW)	Scan Speed (mm/min)
1.5–2.5	300–500
3–3.5	400–800

FIGURE 3
X-ray diffraction profiles of the top surface (a) as received and (b) laser composite surface with chromium carbide (at a power of 2 kW, scan speed of 200 mm/min and powder feed rate of 20 mg/s).

EVALUATION OF PROPERTIES OF THE SURFACE

Evaluation of microhardness

The Microhardness of the laser composite surface with Cr_2C_3 was measured both on the top surface and along the cross sectional plane as a function of laser power and scan speed. The average micro-hardness of the composite layer was increased significantly as compared to that of the as-received MEZ. Figure 5 shows the variation of the average micro-hardness of the top surface of the composite layer with Cr_2C_3 particles. Figure 5 shows that the average micro-hardness decreases with an increase in the applied power, plot 1, firm line; $v = 450$ mm/min and $F_p = 20$ mg/s. This may be attributed to a decreased area fraction of chromium carbide particles at a higher P cf. Figure 2. On the other hand, the average micro-hardness of the surface layer increases with an increase in scan speed cf. Figure 3, plot 2, dotted line; $P = 2.5$ kW and $F_p = 20$ mg/s. Although the area fraction of particles on the surface decreases with an increase in scan speed the increased micro-hardness at a higher scan speed is attributed to an increased grain refinement due to a faster cooling rate. Hence, it may be concluded
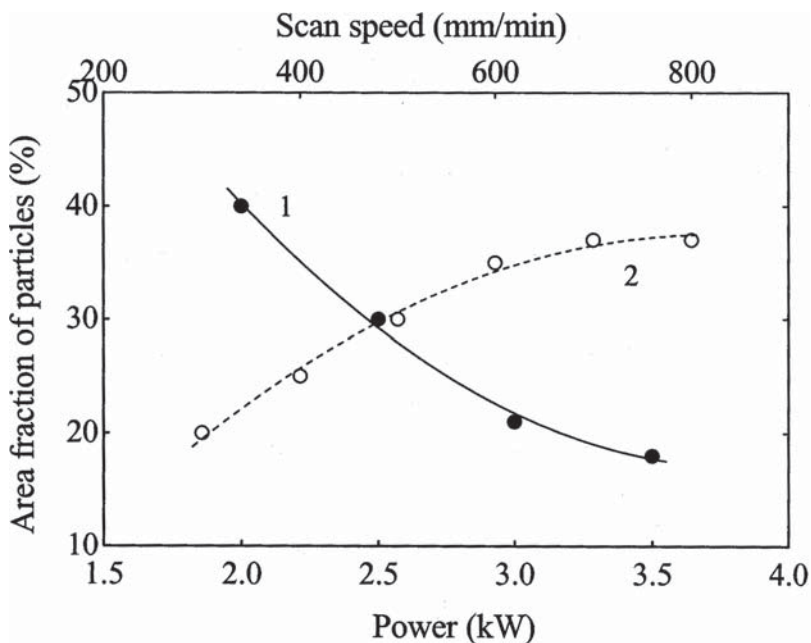

FIGURE 4

Variation of the area fraction of chromium carbide particles in the composite layer of laser composite surfaced MEZ with chromium carbide with applied laser power (graph 1, at a scan speed of 450 mm/min) and scan speed (graph 1, at a power of 2.5 kW).
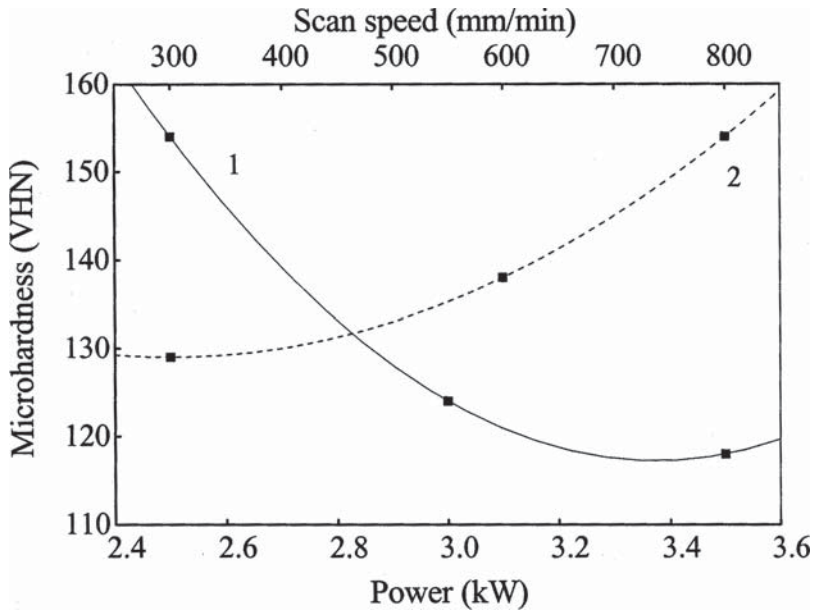
FIGURE 5

Variation of the average microhardness of the top surface of the laser composite surface with chromium carbide with applied laser power (graph 1, at a scan speed of 450 mm/min) and scan speed (graph 2, at a power of 2.5 kW).

that the mechanism of hardening of the laser composite surface Mg is due to a combined action of grain refinement and precipitation hardening.

Evaluation of wear resistance

The wear loss of as-received and the composite surface were measured by a Pin-on-Disc wear testing machine against a hardened steel disc with an applied load of 3 kg and 300 rpm for a period between 1 min. to 3 h, and measuring the wear loss of materials at a regular interval. Figure 6 compares the wear loss of the as-received MEZ, plot 1 and that of the composite surface with Cr_2C_3 at a power of 2.5 kW, scan speed of 450 mm/min, plot 2 as a function of time. It should be noted that both the magnitude and kinetics of wear are significantly reduced as a result of the composite surface. Furthermore, for MEZ the kinetics of wear is predominantly linear in the initial stage and subsequently, reaches a steady state after a prolonged duration, possibly due to presence of worn out debris at the mating surface of substrate and hardened steel disc. On the other hand, the wear rate is significantly reduced for the composite surface with Cr_2C_3 and follows a linear kinetics throughout. The constant rate of wear in the composite surface is attributed to a very low rate of wear
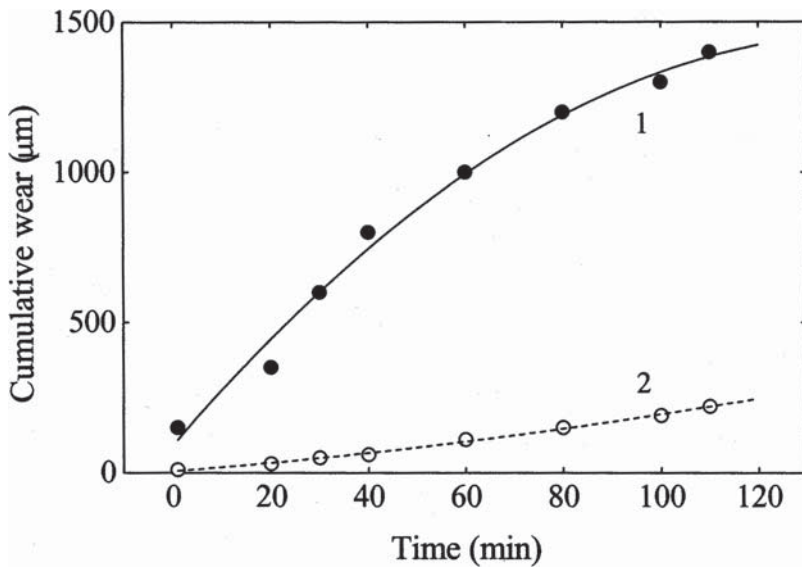
FIGURE 6
Comparison of the wear loss of as-received (plot 1) and the laser composite surface (plot 2) MEZ by a pin-on-disc wear testing machine against hardened steel ball (at an applied load of 3 kg and wheel speed of 300 rpm).

throughout. The improved wear resistance of the laser composite surface is attributed to an improved micro-hardness in the surface layer due to the presence of hard ceramic particles.

Evaluation of corrosion resistance

The effect of composite surfacing on the pitting corrosion behaviour was studied and compared with that of the untreated MEZ by calculating the corrosion rate derived from the potentiodynamic anodic polarization study in NaCl. The Tafels plot was constituted from the logarithm of the current value as a function of voltage [15]. The slope of the Tafels plot in the linear region in the anodic direction is referred to as the anodic Tafel constant and the same in cathodic direction is called the cathodic Tafel constant. The corrosion current (i_{corr}) was determined from the intersection

TABLE 2
Summary of corrosion results for the laser composite surface with Cr_3C_2

Sl. No.	Solution	Corrosion Rate (mpy)	
		As-received	Composite Surfaced MEZ
1	0.5% NaCl	130	27
2	2.0% NaCl	200	72
3	3.56% NaCl	521	100
4	10.0% NaCl	1200	236

of these two linear plots, which is taken as a measure of the corrosion rate. Table 2 compares the corrosion rate of the composite surface with that of the as-received MEZ for a wide range of NaCl solutions.

A detailed comparison of the corrosion rate in the composite surface with that of as-received MEZ shows that the corrosion resistance has been significantly improved in the composite surface. The improvement might be attributed to the super-saturation of the rare earth content in MEZ and grain refinement due to a rapid quenching associated with laser melting [9]. However, the reasons for the improvement of the corrosion resistance due to the laser composite surface has not been investigated in the present study [12].

SUMMARY AND CONCLUSIONS

In the present investigation, a composite surface was produced by dispersing Cr_3C_2 onto the surface and by surface melting MEZ with a high power CW CO_2 laser. The following conclusions may be drawn from the present study:

1. The optimum laser parameters for the formation of a defect-free and homogeneous microstructure are: laser power = 1.5-3.5 kW, scan speed of 300–800 mm/min and powder feed rate of 20 mg/s.
2. The microstructure of the composite surface consists of a uniform, distribution of Cr_3C_2 particles in a grain refined MEZ matrix. The average area fraction of the particles was found to vary from 10–50%. The area fraction of Cr_3C_2 was found to decrease with an increase in the applied power and also an increase in the scan speed, respectively.
3. The average micro-hardness of the composite surface was increased significantly 100–200 VHN as compared to that of 35 VHN of the MEZ matrix. The mechanism of hardening was due to the combined effect of grain refinement and dispersion hardening due to the presence of Cr_3C_2 particles.
4. The wear resistance was significantly improved 4 to 6 times in the composite surface as compared to that of the as-received MEZ. The improved wear resistance of the composite surface was attributed to the improved hardness of the composite surface.
5. The corrosion resistance was improved by the laser composite surface as compared to that of the as-received MEZ.

ACKNOWLEDGEMENTS

REFERENCES

[1] Raynor, G. V. (1959) (Ed.), The Physical Metallurgy of Magnesium and its Alloys. London: Pergamon Press, 1.

[2] Rabinowicz, E. (1965) (Ed.), Friction and Wear of Materials, *John Wiley and Sons,* New York.

[3] Kapat, J. S, Dahotre, N. B., and Sudarshan, T. S. (1999) (Eds.), Chemical Vapor Deposition of Intermetallic and Ceramic Coatings, New York, *Marcel Dekker Inc.,* 441.

[4] Mazumdar, J., and Stern, K. H. (1996) (Ed.), Metallurgical and Ceramic Protective Coatings, London: *Chapman and Hall,* 74.

[5] LE, Rehn, ST, Picraux, and Wiedersich, H (1987) (Eds.), Surface Alloying by Ion, Electron and Laser Beams, Ohio, ASM, Metals Park, 1.

[6] Mordike, B. L., Cahn, R. W., Haasan, P., and Kramer, E. J. (1993) (Eds.). Materials Science and Technology, Weinheim, VCH, 111.

[7] Dutta Majumdar, J., and Manna, I. (2003). *Sadhana, 28,* 495.

[8] Galun, R., Weisheit, A., and Mordike, B. L. (1998). *Corrosion Reviews, 16,* 53.

[9] Dutta Majumdar, J., Mordike, B. L., Galun, R., and Manna, I. *Mater. Sci. Eng., A, (communicated)*

[10] Dutta Majumdar, J., Mordike, B. L., Galun, R., Maiwald, T., and Manna, I. *Lasers in Engineering* (communicated).

[11] Dutta Majumdar, J., Ramesh Chandra, B., Galun, R., Mordike, B. L., and Manna, I. (2003). *Comp. Sci. Technol., 63,* 771–778.

[12] Dutta Majumdar, J., Ramesh Chandra, B., Galun, R., Mordike, B. L., and Manna, I. (2004). *Surf. Coat. Tech., 179,* 297–305.

[13] Hilliard, J. E., Dehoff, R. T., and Rhines, F. N. (1968) (Eds.), Quantitative Microscopy, London, *Mc Graw-Hill Book Company*; 45.

[14] Standard Practice for Conducting Cyclic Potentiodynamic Polarization Measurements for Localized Corrosion, ASTM Standards. 1961:G61.

[15] Fontana, M. G. (1987) (Ed.), *Corrosion Engineering. New York, McGraw-Hill.*